AIAA Journal
Vol. 48, No. 7, July 2010

Efficient Topology Optimization of Large Dynamic Finite Element Systems Using Fatigue

Karim Sherif*
Linz Center of Mechatronics, 4040 Linz, Austria
Wolfgang Witteveen† and Klaus Puchner‡
Magna Powertrain, ECS, 4300 St. Valentin, Austria
and
Hans Irschik§
Johannes Kepler University, 4040 Linz, Austria

DOI: 10.2514/1.45196

The present paper modifies and extends the recently developed equivalent static load method for the optimization of dynamically loaded linear elastic finite element systems with a huge number of degrees of freedom. In the equivalent static load method, dynamic loads have been transformed into equivalent static loads. This leads to an equivalent static response optimization with multiple loading conditions instead of a dynamic optimization problem. In the present paper, the equivalent static load algorithm is modified and extended by introducing a fatigue analysis in the iterative optimization procedure, where damage is used as suitable termination criterion of the iteration, as well as for the determination of a single and meaningful equivalent static load that leads to maximal damage in the structure. During the evolution process the structure is systematically stiffened by using the solid isotropic microstructure with penalization approach until a user-defined damage level is reached. Three standard examples from literature and an industrial application with a large number of degrees of freedom (600,000) demonstrate the computational efficiency of the proposed method.

I. Introduction

TOPOLOGY optimization has been developed to optimize the material distribution within a fixed design domain for a structure with a given set of constraints and loads. Because of the economically driven requirements of increasing product quality and decreasing product costs, topology optimization has gone through an extensive development. Particularly in the framework of the finite element formulation, various different optimization methods have been published in the last decades.

Several methods are either based on the homogenization (microstructure) approach, originally described by Bendsøe and Kikuchi in 1988 [1] or on the so-called solid isotropic microstructure with penalization (SIMP) approach, introduced by Bendsøe in 1989 [2]. The SIMP, or power law approach, does not use discrete microstructures, but rather a continuous design parameter b_i ($0 \leq b_i \leq 1$) that represents the relative mass density of each finite element. Furthermore, Young's modulus of each finite element is given as its relative density raised to some power, times the reference Young's modulus [3,4]. In the following years, different approaches have been published, following either the homogenization method [5,6] or the SIMP approach [7,8]. A comprehensive review has been published by Eschenauer and Olhoff [9].

A common motivation for optimization in automotive, aerospace or aircraft industry is the reduction of weight. A lighter structure tends to have lower natural eigenfrequencies, which are more easily excited under common loading conditions. Therefore, it may be essential to regard inertia effects during the optimization procedure of dynamically loaded components. One of the earliest approaches on structural optimization under dynamic loads has been introduced by Fox and Kapoor [10]. In the latter approach, a minimum-weight problem is formulated together with certain constraints on deformation and stresses. Diaz and Kikuchi [11] proposed a solution strategy for the maximization of the fundamental frequency, which is based on the homogenization method. The problem is formulated as a reinforcement problem in which a given structure is stiffened by additional material.

To avoid the high computational effort of a direct mathematical optimization in a dynamic response optimization problem, the concept of equivalent static loads has been introduced in the literature (see, e.g., [12–14]). The basic idea of the latter concept is the transformation of dynamic loads into a series of equivalent static loads (ESL). This leads to a static response optimization with multiple loads instead of a dynamic response optimization, for which second-order algebro-differential equations would have to be solved. Kang et al. [15] have linked this concept to flexible multibody dynamic simulations, which leads to an iterative structural optimization procedure of dynamically loaded elastic components with an acceptable computational effort.

However, the latter publication concluded with some doubts, whether the procedure could be applied to huge structures. In the present paper, we propose an efficient algorithm for structural optimization of huge and dynamically loaded FE models, which can be integrated in multibody dynamic systems (MBS) in a straightforward manner. Large FE models are needed in case of complex design spaces with given edges, bores, and the like, as this is common for advanced applications in industry. The presented method is derived from the ESL approach, but, instead of a stress constraint, a damage constraint is applied, which leads to several advantages: Damage can be used as a quite natural termination criterion in the iterative procedure of an optimization process, due to the fact that it integrates the effects of load induced stress over the time, and it is a proper value for the indication of structural failure. Moreover, and this is the main point in our presentation, the area with

Received 30 April 2009; revision received 11 January 2010; accepted for publication 31 March 2010. Copyright © 2010 by the American Institute of Aeronautics and Astronautics, Inc. All rights reserved. Copies of this paper may be made for personal or internal use, on condition that the copier pay the $10.00 per-copy fee to the Copyright Clearance Center, Inc., 222 Rosewood Drive, Danvers, MA 01923; include the code 0001-1452/10 and $10.00 in correspondence with the CCC.

*Junior Researcher, Multi-Body and Multi-Field Dynamics; karim.sherif@lcm.at.

†Senior Researcher, Dynamics/Acoustics; wolfgang.witteveen@ecs.steyr.com.

‡Development Engineer, Durability/Suspension; klaus.puchner@ecs.steyr.com.

§Professor and Head, Institute of Technical Mechanics; irschik@mechatronik.uni-linz.ac.at. Member AIAA.

the highest damage value gives a criterion for a single and meaningful ESL. In this respect, we will use the mode-based approach of the FE method, together with an effective method for the damage analysis. In the present contribution we use the commercial codes MSC.Adams [16] and FEMFAT [17] (see Sec. II.C for details). In contrast to a costly global optimum search, in the following the SIMP approach [18] is used for a systematic reinforcement of the structure until a desired damage level is obtained. The disadvantage of not having a mathematical proof for a strictly global optimum thereby should be compensated by the excellent computational efficiency. Because of the fact that the content of the present contribution does not provide a new set of formulas, but a novel and advantageous combination of existing methods, the first section of our paper gives a short review of the three key methods, on which the proposed method is based. In the next section, the problem description is illustrated in detail, and a flowchart of the proposed algorithm is presented. The paper ends with four numerical examples. One generic example is given for the sake of illustration. Another example, which is taken from [15], is retreated in order to show the significant increase of lifetime of an optimized FE structure, which is integrated in a multibody system. In a third example, the proposed algorithm is compared to an alternative method known from the literature [11], where the optimization objective was the global search of the maximum of the first eigenvalue. Finally, a successfully optimization of a FE model of a dynamically loaded vehicle frame component with a complex design space [600,000 nodal degrees of freedom (DOF)] gives further evidence for the efficiency of the procedure.

II. Brief Review on the Three Key Methods of the Proposed Algorithm

A. Brief Review on the Equivalent Static Load

The equation of motion of a FE model can be formally written as

$$M(b)\ddot{y}(t) + K(b)y(t) = r(t) \tag{1}$$

where M and K are the $(n \times n)$ mass and stiffness matrices, which depend on the $(e \times 1)$ design variable vector b representing the relative mass density of each finite element. The $(n \times 1)$ vector $r(t)$ represents the time-varying external load, t denotes the time, and the $(n \times 1)$ vector y contains the nodal DOF (usually displacements) of the FE model. The $(n \times 1)$ vector $\ddot{y}$ is the second derivative of y with respect to time. The scalar quantities n and e represent the number of nodal DOF and elements of the FE model, respectively. The FE formulation (1) can be incorporated into MBS codes in a standard manner, which allows us to restrict ourselves in the following to the simple form presented in Eq. (1).

By performing a discretization of the time interval of interest $[0, T]$ into q time grid points, Eq. (1) can be rearranged to

$$K(b)y_u = r(t_u) - M(b)\ddot{y}_u, \qquad u = 1, \ldots, q, \qquad t_1 = 0, \qquad t_q = T \tag{2}$$

The index u represents the number of the time grid point. As a result of a transient analysis, the displacement vector y_u is known at each time grid point t_u. Using the definition that the ESL induces the same displacement field in a flexible body as would be induced by a dynamic load at a certain time, the $(n \times 1)$ ESL vector at time t_u, f^u_{eq}, can be obtained as

$$f^u_{\mathrm{eq}} = K(b)y_u, \qquad u = 1, \ldots, q \tag{3}$$

where the displacement vector y_u, which is already known due to the transient analysis, is substituted. In contrast to the external load vector $r(t)$, which typically acts at a few nodes of the FE model only, the ESL is a distributed load, which acts on the entire structure. That is, the ESL is applied to all degrees of freedom of the structure and can only be obtained after having performed a transient analysis of the structure. Since the time interval of interest is divided into q time grid points, after the transient analysis q displacement fields y_u are known $u = 1, \ldots, q$ [see Eq. (3)]. According to Eq. (3), it is possible to compute for each displacement field y_u the corresponding equivalent static load f^u_{eq}, from which the most damaging will be selected for optimization (see below). Thus, the objective of the ESL is the static generation of a known displacement vector caused by dynamics during an optimization procedure. For a more detailed description of the underlying ESL method, the reader is referred to [13,19].

B. Brief Review on the Static Optimization Using the SIMP Method

The SIMP method was proposed under the term *artificial density approach* by Bendsøe [2] over two decades ago. This method assumes that Young's modulus and the density of each finite element can be used as intermediate design variables. The most significant advantage of the SIMP method is its computational efficiency in terms of CPU time, since only one free variable is used per element. The SIMP formulation is based on the minimization of the total compliance C (the maximization of the overall stiffness) with respect to a volume constraint. This can be formulated as

$$\min_b \; C(b) = y^T K(b) y \tag{4}$$

subject to

$$K(b)y = r \tag{5}$$

with the constraints

$$\sum_{i=1}^{e} b_i V_i - V_{\mathrm{end}} \leq 0, \qquad (V_{\mathrm{end}} = \beta V_\Omega), \qquad (0 < \beta < 1) \tag{6}$$

$$0 < b_i \leq 1 \tag{7}$$

where the symbols b_i and V_i are the relative mass density and the volume of element i, respectively, and β denotes the volume fraction of available material and is given by $V_{\mathrm{end}}/V_\Omega$, where V_Ω is the volume of the admissible design domain Ω. A detailed description of the formulation described above can be found in [20]. Pedersen [21,22] showed that the minimum compliance problem [Eqs. (4–7)] is equivalent to a structural optimization, which targets a uniform stress distribution within the optimized structure.

C. Brief Review on Fatigue Analysis

For introducing fatigue analysis, the damage parameter according to Lemaitre [23] is adopted. In the latter publication, a scalar value D was introduced for a representative volume element (RVE) at an arbitrary structural point. The value of D is bounded by zero and one, where $D = 0$ in the undamaged RVE, and $D = 1$, if the RVE material is fully damaged. Furthermore, a material depending critical damage value D_c is introduced, which defines the initiation of microcracks. Increased loadings tend to enlarge an existing microcrack and this will finally lead to the rupture of the whole RVE. For different reasons it is not advantageous to use the damage parameter D for structural optimization. The computation of crack propagation in the framework of FE analysis is quite complex, and in many technical applications an existing microcrack already must be interpreted as structural failure. Moreover, it seems not to be necessary to incorporate the crack propagation at the early design stage, in which topology optimization is applied. Therefore, for the subsequent studies, a normalized damage parameter $D_{c,n}$ is introduced that is defined as

$$D_{c,n} = \frac{D}{D_c} \tag{8}$$

For the proposed topology optimization technique the relevant range of $D_{c,n}$ is delimited by zero and 1. Consequently, $D_{c,n} = 0$ characterizes an undamaged structure and $D_{c,n} = 1$ indicates local crack initiation. A value in between these boundaries ensures that structural failure will not occur.

For the fatigue analysis, the commercially available software package FEMFAT [17] is used subsequently. The latter software computes $D_{c,n}$ for each node of the FE structure. The fatigue software

FEMFAT is based on the linear accumulation of damage fatigue following the Palmgreen–Miner rule (see [23–25]). Because the focus of this presentation is on topology optimization using fatigue and not on fatigue itself, just a brief review on the latter fatigue concept is given next. For a comprehensive presentation of how the latter method is implemented in FEMFAT, the reader is referred to [17,26,27].

1) In a first step, FEMFAT imports the FE model of a structure, the FE stress distributions due to certain loads, load histories, and material data.

2) In a next step, synthetic SN curves are computed for each node of the FE model. The term synthetic means that a SN curve, which is gained by mechanical experiments with standardized specimen, is automatically adapted according to local parameters like mean stress, notches, material temperature, and others. This SN curve holds a relationship between the endurable number of load cycles until a crack is initiated and an according stress amplitude.

3) Based on the imported stress distributions and the according load histories a time-varying stress is computed for each node of the FE structure.

4) For the computation of a damage value according the Palmgreen–Miner rule the theoretical endurable number of load cycles from the SN curve of step 2 is compared with the actual counted load cycles at a certain stress amplitude from step 3. This is done for each FE node of the structure.

It is emphasized that any other software capable of computing a reduced damage parameter could be used in the present methodology. It is furthermore noted that damage has been suggested for static topology optimization problems by Dannbauer et al. [28] (see also [29]). The present paper represents an extension to dynamic topology optimization for large FE models. A preliminary formulation has been presented by the first author in [30].

The efficiency of the transient fatigue analysis is dependent on the quality of flexible body's representation in the FE models. Typically, the deformations of the FE model are computed by a linear superposition of a suitable set of Ritz vectors, commonly called modes. Formally, this can be written as

$$y(t) = \Phi s(t) \tag{9}$$

where the modes are collected in the $(n \times m)$ modal matrix Φ and the time-varying scaling factors are collected in the $(m \times 1)$ vector $s(t)$. The number of considered modes is m. The stress state at each time t, which is relevant for the fatigue analysis, can be efficiently reconstructed by a superposition of modal stress shapes (see [31]). The scaling factors for the resulting stress and deformation are identical [namely, $s(t)$], and they are a result of the time integration. This can be expressed as

$$\sigma = E\Gamma y = E\Gamma\Phi s(t) = \sum s(t) \tag{10}$$

where the $(w \times 1)$ vector σ corresponds to a vector representation of the stress tensors of the relevant finite elements, E represents a matrix representation of the elasticity tensor, Γ contains differential operations necessary for computing the strains. Note that all matrices can gathered in the $(w \times r)$ matrix Σ, which contains r modal stress shapes. The matrix Σ is typically a byproduct of the FE analysis, which is necessary anyway in order to compute the modal deformation shapes Φ.

From the point of view of FEMFAT, the necessary stress distributions are given by Σ and the required load histories are given by $s(t)$.

III. Proposed Dynamic Response Optimization for FE Models Using Fatigue as Key Quantity

A. Some Motivation for the Use of Damage in the Optimization Procedure

The presented research was originally motivated by the absence of a method for efficient topology optimization of huge FE models undergoing dynamic loads by means of commercially available software packages. To the best knowledge of the authors, the topology optimization procedures known from the literature are not capable for these kinds of problems, mainly due to the huge CPU time that is needed. These methods for dynamic topology optimization are typically characterized by the use of certain stress restrictions as termination (constraint) criteria in the iterative procedure. But in structures, which are subjected to dynamic loads, the stresses will vary with respect to time, and so the stress constraint has to be satisfied over the entire time range. An attractive alternative reducing the computational effort is to replace the time-varying constraint by damage, because it takes into account the entire load history in an integrative manner [24]. The integration of a damage restriction into the topology optimization procedure instead of stress is a key feature of the proposed method and leads to an algorithm, which can be efficiently used for large structures and long time series. A qualitative comparison of a stress restriction based approach and the proposed damage restriction based approach is given in Table 1.

In general, a dynamic optimization problem can be written as

$$\min_b \varphi(b) \tag{11}$$

subject to

$$M(b)\ddot{y}_u + K(b)y_u = r(t_u), \qquad u = 1, \ldots, q \tag{12}$$

with the constraints

$$g_{ju}(b, y_u, \ddot{y}_u) \leq 0, \qquad j = 1, \ldots, k, \qquad u = 1, \ldots, q \tag{13}$$

where $\varphi(b)$ represents a cost function, and g_{ju} is the jth constraint at the uth time grid point. In contrast to static response optimization, where algebraic equations need to be solved, dynamic response optimization leads to differential-algebraic equations of second order. A direct solution of the latter equation is economically not possible for a large number of DOF. This is a strong restriction due to the fact that given design spaces can be geometrically very complex because of given edges, bores, and the like.

However, for solving the general dynamic response optimization problem [Eqs. (11–13)], the algorithm introduced by Choi and Park [14] can be used. In the latter algorithm, the differential-algebraic

Table 1 Comparison of a stress restriction based approach and a damage based restriction approach

Stress as a constraint	Damage as a constraint
Stress characterizes just one time instant.	Damage integrates the entire load history because it characterizes how the stress effects a structure.
Stress is a quantity that needs to be interpreted carefully. Consequently, the most stressed area may not necessarily be the most critical area.	Damage is a meaningful quantity that summarizes the stress level, load history, material properties, local characteristics, etc.
In case of several time steps with comparable maximum stress distributions, several ESL need to be considered, which leads to a static topology optimization with multiple loads.	The damage analysis enables the determination of one meaningful ESL. This leads to a static topology optimization with only one single load case.
The iterative optimization procedure is terminated in case of a converged material distribution. This may be a costly requirement.	Because of the fact that a damage value smaller than 1 ensures the absence of structural failure, damage can be used directly as natural termination criterion.

equations are transformed into algebraic equations by the use of the previously introduced ESL method (see Sec II.A). This method leads to a series of static optimization problems with multiple loading conditions. It has been verified by Park et al. [32] that the solution obtained satisfies the necessary Karush–Kuhn–Tucker conditions and is an optimum solution of the original dynamic response optimization.

In the present paper, our goal is the minimization of the volume of a structure, using an upper bound for damage D_{user} as a constraint. Formally, this can be written as

$$\min_{b} V(b) \tag{14}$$

subject to

$$M(b)\ddot{y}_u + K(b)y_u = r(t_u), \qquad u = 1, \ldots, q \tag{15}$$

with the constraint

$$\forall\ x \in N\colon D_{c,n}(x, T) \leq D_{\text{user}}, \qquad D_{\text{user}} \ll 1 \tag{16}$$

where V represents the volume depending on the volumetric material densities of each element, which are collected in the relative design variable vector b. The constraint of the optimization problem is given by the inequality Eq. (16), where $D_{c,n}(x, T)$ is the normalized damage value at the node number x of the structure at time T, and D_{user} is a user-defined upper bound for damage. For practical situations, the user will select $D_{\text{user}} \ll 1$ for safety reasons. N represents the subset of all FE nodes that are evaluated with respect to fatigue. By using a user-defined upper bound for damage, the lifetime of the generated structure is automatically ensured. Compared to stress constrains, which have to be satisfied over the given range of time, the damage constraint of the optimization is easy to handle.

Instead of a global optimum search of the cost function, an iterative procedure is suggested, where each optimization cycle represents a SIMP optimization with a given end volume

$$V_{p+1} = V_p + \beta_{p+1} V_\Omega \tag{17}$$

In the subsequent examples, the commercial code TOSCA [33,34] has been used for the SIMP optimization. For a more detailed description of the underlying SIMP technique, the reader is referred to [2,7,8,18,35,36]. It is emphasized that any other computer code capable for the SIMP-computation could have been used instead of TOSCA.

The index p represents the optimization cycle number. Thus, the pth cycle can be written as

$$\min_{b} C(b_{p+1}) = y^T \cdot f^u_{\text{eq},p} \tag{18}$$

subject to

$$K(b_{p+1})y = f^u_{\text{eq},p} \tag{19}$$

with the constraints

$$\sum_{i=1}^{e} b_i V_i - V_{p+1} \leq 0, \qquad (V_{p+1} = V_p + \beta_{p+1} V_\Omega) \tag{20}$$

$$0 < (b_i) < 1 \tag{21}$$

This procedure has to be iteratively repeated with a successive increasing end volume V_{p+1} and an adopted ESL $f^u_{\text{eq},p}$, until $D^p_{c,n}(x, T) \leq D_{\text{user}}$ for all nodes x of the set N. This can be interpreted as a systematic reinforcement of the structure, by adding in each optimization cycle the predefined amount of material $\beta_{p+1} V_\Omega$, until the defined damage level is reached. The next paragraph is devoted to the open issue of defining the ESL $f^u_{\text{eq},p}$.

Note that after the transient analysis of the pth structure, the stress field history $\sigma_{e,p}(x, t_u)$ is given for all time grid points $u = 1, \ldots, q$. Based on this, the structural normalized damage values of the pth optimization cycle $D^p_{c,n}(x, T)$ can be computed for each node x of the set N. The critical node x_c is the node with the highest damage and can be determined as

$$D^p_{c,n}(x_c, T) = \max_{x}(D^p_{c,n}(x, T)), \qquad x \in N, \rightarrow x_c \tag{22}$$

For the determination of the critical time grid point $t_{u,c}$, the equivalent stress, on which the damage computation is based, is evaluated at node x_c as

$$\sigma_{e,p}(x_c, t_{u,c}) = \max_{t_u}(\sigma_{e,p}(x_c, t_u)), \rightarrow t_{u,c} \tag{23}$$

The ESL that generates the significant critical displacement field with respect to damage is consequently defined as

$$f^u_{\text{eq},p} = K(b_p) y_{u,c} \tag{24}$$

This single ESL is necessary to characterize the already known critical displacement field during a static optimization procedure. Since, there is one critical time grid point, there is only one critical displacement field in each iteration: namely, that which causes the highest damage to the structure. It is worth mentioning that the location and the time where and when the highest damage occur can change during a dynamic simulation, but it is clearly defined when the entire simulation time is evaluated in terms of fatigue damage. However, by performing a static optimization procedure as described in Eq. (18–21), in which the latter single ESL is used as a design-oriented static load, the topology of the structure changes by adding material in order to stiffen the structure. If the user-defined damage level is not achieved, another iteration (optimization cycle) has to be performed. This yields, due to the change of the topology of the structure, a different critical displacement field and thus, after each static optimization cycle, in which the structure is reinforced by adding a predefined amount of material, the single ESL of Eq. (24) has to be updated.

B. Flowchart of the Proposed Damage-Based Optimization Process

Subsequently, we give a flowchart of the proposed algorithm:

Step 1: Set $p = 0$ and b_0. Define V_0, D_{user}, V_Ω, and the set N.

Step 2: Generate a base structure with the end volume V_0 by solving an optimization problem with representative static loads.

Step 3: Compute the structures modes Φ and σ, the corresponding modal stress distribution [Φ and σ according to Eqs. (9) and (10)].

Step 4: Based on the displacement mode shapes of step 3, a transient dynamic analysis is performed, which gives the modal participation factors $s(t)$ as a result.

Step 5: Based on the stress distributions of step 3 and the modal participation factors of step 4, a mode-based fatigue analysis is performed.

Step 6: If

$$\forall\ x \in N\colon D_{c,n}(x, T) \leq D_{\text{user}} \tag{25}$$

then stop.

Step 7: Determine the critical time grid point $t_{u,c}$ for the significant ESL according to Eq. (23).

Step 8: Determine the significant equivalent static load with respect to damage according to Eq. (24).

Step 9: Define β_{p+1}.

Step 10: Determine a reinforced structure by solving a static response optimization problem according to Eqs. (18–21).

Step 11: Set $p = p + 1$, and go to step 3.

For the sake of clarity, step 2 is described in the following in more detail. The generated base structure of step 2 needs to be an undersized structure, due to the fact that in each optimization cycle material is added. This undersized structure has not to be necessarily generated by solving an optimization problem with representative static loads as described in step 2 of the proposed algorithm, but rather can be a given core structure as it is demonstrated in the third example of the next section. Another approach for the determination of the core structure would be the solution of a static optimization problem with representative static loads as it is demonstrated in the first example of Sec. IV. From the external load vector

$$r(t) = \{r_1(t), \ldots, r_i(t), \ldots, r_n(t)\}^T, \qquad i = 1, \ldots, n \tag{26}$$

a representative static load vector r_{rs} can be defined as

$$r_{\mathrm{rs}} = \{\max_t(r_1(t)), \ldots, \max_t(r_i(t)), \ldots, \max_t(r_n(t))\}^T \qquad i = 1, \ldots, n \tag{27}$$

Obviously, several strategies can be applied to achieve a core structure.

From step 3 to step 11, one optimization cycle is completed. The procedure is executed and the structure is systematically reinforced until the user-defined damage level is achieved.

In contrast to the original conceptual formulation [see Eqs. (14–16)], where the volume of the structure has been minimized, the presented procedure (see step 3–step 11) reinforces the base structure of step 2 by adding a predefined amount of material $\beta_{p+1} V_\Omega$ in each optimization cycle. Thus, the solution does not necessarily represent the lightest possible structure, but this can be accepted due to the overall efficiency of the procedure, which is demonstrated in the following numerical examples.

IV. Numerical Example

Four examples will be presented to illustrate the proposed algorithm, to compare the results with the literature, and to show its efficiency in the framework of an industrial application. In the first example, an optimization of a simple two-dimensional plate problem is presented in order to get a general overview of the flow of the optimization process. This example demonstrates that the presented algorithm can handle dynamic systems, in which more than one natural frequency is exited. The second example deals with the optimization of a single bar, which is integrated in a multibody system four-bar mechanism. The latter example is taken from [15]. Although the objectives of the optimization tasks are different from [15], the subsequent results illustrate the potential of the proposed topology algorithm. Finally, a vehicle frame component with a large number of degrees of freedom is successfully and efficiently optimized. Even for the large problem, the optimization process leads to a comparatively low computational effort.

A. Two-Dimensional Plate Problem

A rectangular structure, which is supported at the left upper and left lower corners, is loaded by a point load of sine wave type, which is applied on the top right corner (see Fig. 1). The sine wave is defined as a sweep, where the amplitude is constant (15,000 N), and the frequency increases linearly with respect to time from 400 to 1000 Hz. Consequently, all structural modes of the frequency band are exited. The FE model of the design domain (300 × 150 mm) consists of 7200 four-node plane quadrilateral finite elements with 7381 nodes. Furthermore, the design domain is filled by a homogenous isotropic iron type material with Young's modulus of $210{,}000\ \mathrm{N/mm^2}$, Poisson's ratio of 0.3 and a mass density of $7850\ \mathrm{kg/m^3}$. For the overall mode-based dynamic response computation, an overall modal damping ration of 1% has been used, and the necessary parameters to be predefined for the optimization have been defined as

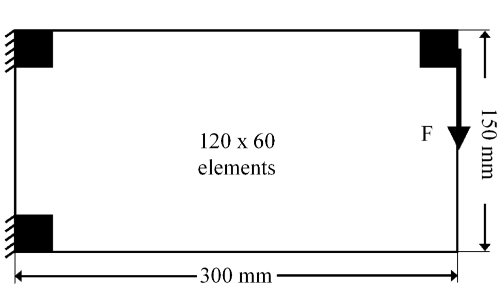

Fig. 1 Design space and boundary conditions/loadings of example 1.

$$b_{p=0} = 7850\ \mathrm{kg/m^3}, \quad V_0 = 0.2 \cdot V_\Omega, \quad \beta_1 = \beta_2 = \beta_3 = 0.025$$
$$D_{\mathrm{user}} = 0.1, \quad T = 0.5\ \mathrm{s}, \quad q = 10000$$

After three cycles the optimization process is successfully terminated and the computed design occupies 27.5% of the original design domain. Table 2 contains the evolution history of the structure according to the optimization cycle. The proposed optimization procedure is briefly visualized in the images in Table 2. At the zeroth optimization cycle, a core structure is generated by performing a static topology optimization. Using the Eq. (27), the representative static load of the latter optimization is simply a constant point load with amplitude of 15,000 N, which is applied on the top right corner. The resulting structure has two natural frequencies in the frequency band of interest: namely, at 493 and 963 Hz. Both of them are excited during the dynamic response computation, but the second one is determined as the critical one with respect to damage. Consequently, an ESL has been determined that reproduces the displacement field of the second eigenform. The subsequent static optimization based on the latter ESL, with an additional 2.5% available material delivers the structure outlined in the second line of Table 2. This structure has its first natural frequency at 515 Hz, which leads to another optimization loop and to the structure in the third row of Table 2. There is again a structural eigenform at 953 Hz, which requires an additional optimization cycle. The final structure has its first natural frequency at 1399 Hz, which is no longer in the frequency band of excitation. The dynamic response computation together with the modal based fatigue analysis delivers a maximal normalized damage value (less than 0.1), which leads to a successfully termination of the topology optimization process. The optimization process is repeated with different values for β_p and the resulting topologies of the optimized structures are quite similar. This yields to the conclusion that the optimization process is stable.

B. Four-Bar Mechanism

This test problem is taken from [15]. A four-bar mechanism, shown in Fig. 2, consists of three flexible links that are connected to each other and the ground by rotational joints. The three links have a mass density of $2757\ \mathrm{kg/m^3}$ and Young's modulus of $68950\ \mathrm{N/mm^2}$. The length of link 1 (l_1), link 2 (l_2), link 3 (l_3) and link 4 (l_4) are 0.3048, 0.9144, 0.762, and 0.9144 m, respectively. Link 1 rotates at a constant angular velocity ω of $10\pi\ \mathrm{rad/s}$. The goal of the optimization in [15] was to minimize the mass of the mechanism by varying the diameters of the three links, with the bending stress constrained to a maximum of $27.58\ \mathrm{N/mm^2}$.

In contrast to the latter optimization, we consider a reinforcement problem for link 2. The dynamic excitation of link 2 is due to the fact that link 2 is included in a multibody system simulation. Hence, the first natural frequency of link 2 is excited. Note that the approach in [15] and the present one are quite different. Therefore, this example is not intended to be a comparison, but an illustration of the characteristics of the presented algorithm.

The optimized diameter values of link 1 and link 3 have been taken over from [15] as 33.5 and 16.9 mm, respectively. An important difference is that the links here are not modeled by some beam elements, but with a considerable number of hexahedra elements. The initial diameter for the first optimization cycle and the designable domain of link 2 are 4.7 and 35 mm, respectively, and are shown in Fig. 3. The FE model of the design domain is generated by using 103,500 hexahedra elements, which leads to 103,500 DOF for the optimization procedure and to 650,072 nodal DOF for the FE analysis. The flexible multibody dynamic analysis is performed by using the first 20 normal modes. The number of load cycles for the damage analysis is based on the assumption that the operating time of the mechanism is 10 years.

During three optimization cycles material is added and a representative cross section can be seen in Fig. 4. Note that the cross section is varying along the longitudinal axes of the link. The generated structure tends towards a beam with an I cross section, which has to be expected due to the fact that the critical mode is the

Table 2 Evolution history of the structure in example 1

Cycle no.	Optimized structure	$D_{c,n}$	Excited and damage-relevant mode	Mode no.	Frequency of mode, Hz
0		$\gg 1$		2	963
1		$\gg 1$		1	515
2		$\gg 1$		1	953
3		<0.1	——	——	——

first bending mode. Because the presented algorithm and the one of [15] are different, it is impossible to compare both results directly. However, the evolution of the structural damage versus the structural mass can be seen in Table 3. An advantage of the proposed algorithm is that the material is stressed more uniformly than in [15]. This leads to a large damage reduction by a factor 36,682. However, we deal with the same structural mass, and the lifetime of the mechanical structure has consequently been increased specifically. The total number of needed cycles (three cycles) is smaller than that in [15]. Furthermore, during the three cycles, the total number of inner iterations was 15.

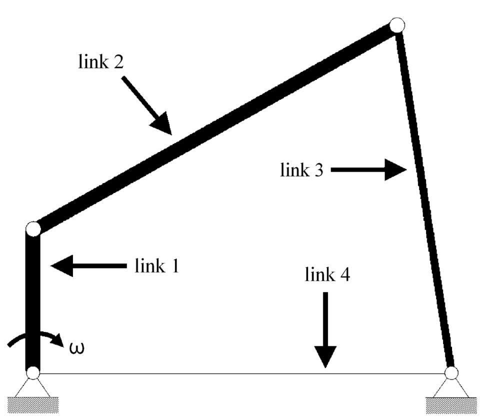

Fig. 2 Damage constrained four-bar mechanism.

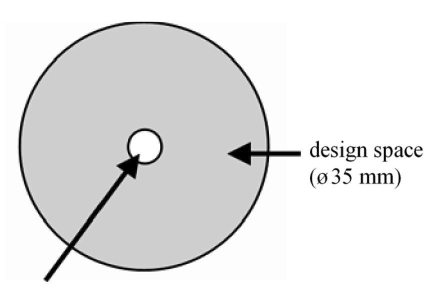

Fig. 3 Cross section of the given structure and the designable domain of link 2.

Even though the optimization has to deal with about 10^5 DOF and the MBS dynamics is fully considered, the computational time is comparatively low. The optimization needed about 6 h CPU time on common computers.

C. Two-Dimensional Two-Bar Truss Structure

The proposed algorithm is applied to the first example treated in Diaz and Kikuchi [11]. The target in [11] was the global maximization of the first natural frequency of the given structure by adding a prescribed amount of material as reinforcement. As outlined

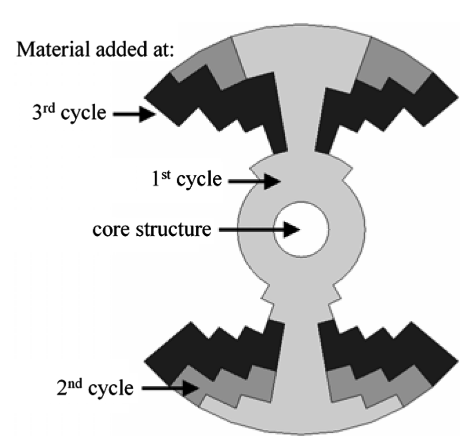

Fig. 4 Representative cross section of the optimized structure.

Table 3 Comparison of the optimization results with the result of [15]

No. of cycles	Mass, kg	$D_{c,n}$	No. of inner iterations
	Proposed algorithm		
0 (core structure)	0.04356	$\gg 1$	15
1	0.5047	3.84	15
2	0.7637	1.52e − 05	15
3	1.0659	2.17e − 07	15
	[15]		
16	1.0657	7.96e − 03	22

Table 4 Comparison with results from Diaz and Kikuchi [11]

Design space added			
6.4%	11.4%	21.4%	31.4%
Proposed algorithm			
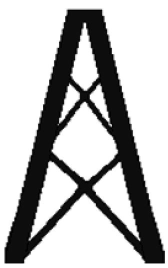			
$\lambda_1 = 6.5\lambda_0$	$\lambda_1 = 7.6\lambda_0$	$\lambda_1 = 9.5\lambda_0$	$\lambda_1 = 10.8\lambda_0$
Diaz and Kikuchi [11]			
$\lambda_1 = 4.0\lambda_0$	$\lambda_1 = 7.8\lambda_0$	$\lambda_1 = 8.7\lambda_0$	$\lambda_1 = 12.0\lambda_0$

in Fig. 5, a given structure (dark elements) is surrounded by the rectangular design space (light elements), which can be used to maximize the first natural frequency. The original structure occupies 23.6% of the (1000 × 1600 mm) domain. As mentioned above, in this example, a core structure is already given, and therefore step 2 of the flowchart of the proposed algorithm has been omitted. In contrast to the procedure of [11], a relevant ESL needs to be computed. Exciting the first natural frequency of the given structure leads to an ESL, which exactly represents the first eigenmode (see Fig. 6).

Analogous to [11], various amounts of material have been provided for the optimization (6.4–31.4% of the design domain). The results are summarized in Table 4. For a comparison, the reader is referred to Fig. 7 of Diaz and Kikuchi [11]. The first eigenvalue of the given structure is denoted as λ_0 and λ_1 is the first eigenvalue of the reinforced structure.

It is demonstrated in Table 4, that the resulting topologies and eigenvalues of the proposed algorithm are different from the results presented in Fig. 7 in [11]. Possible reasons are:

1) A systematic difference between [11] and the presented approach is the different discretization of the design space. Because of the finer discretization in the presented work (a grid of 160 × 100 elements was used) thinner trusses can be achieved as with the grid of 64 × 40 elements, which has been used in [11].

2) Another remarkable difference between [11] and the presented approach is the usage of completely different optimization strategies. The explicit main goal in [11] is the maximization of the first natural frequency by changing the topology of a given structure by adding a prescribed amount of material. In contrast, the target of the presented algorithm is a structural reinforcement until a user-defined damage level is obtained.

However, it is remarkable that in some cases a higher λ_1 is achieved than in [11].

D. Vehicle Frame Component

An industrial application has been chosen to underline the efficiency of the proposed topology optimization method for large

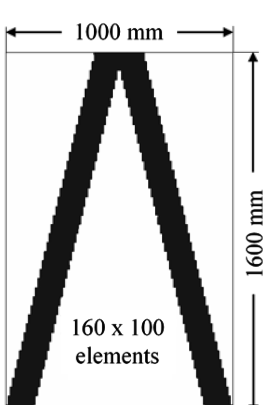

Fig. 5 Given structure and the designable domain.

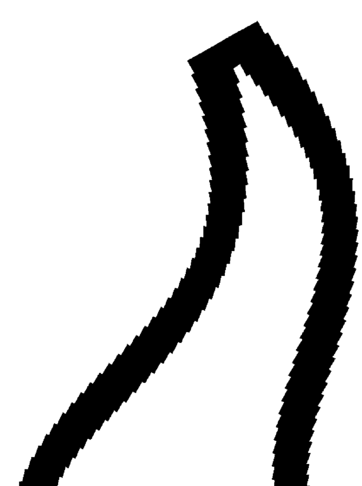

Fig. 6 First natural mode.

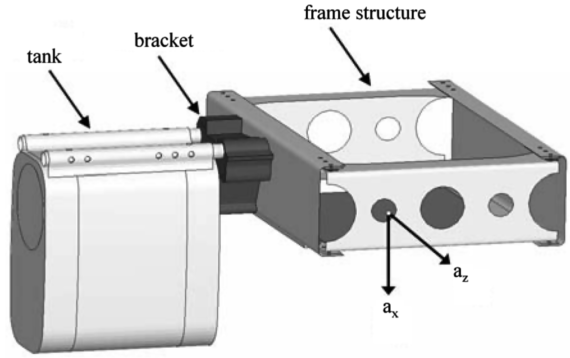

Fig. 7 Entire original model.

and complex FE models. The FE model under consideration represents a virtual test bench for a vehicle component; see Fig. 7 for an image of the entire structure. A tank is connected to a frame structure via a so-called bracket. The frame is mounted on a vibrating table that imposes lateral and vertical accelerations on the frame, which leads to tensions in the bracket due to the inertia of the tank. The goal of this optimization is the computation of a bracket with a damage level below 0.001 by minimum weight.

The available design space is outlined in Fig. 8. A FE model of the design domain is generated by using 180,450 hexahedra elements, which leads to 180,450 DOF for the optimization procedure and to 587,979 nodal DOF for the FE analysis. However, the number of nodal DOF of the full FE model is 1.4e + 6. Furthermore, the design domain is filled by a homogenous isotropic material, where the properties of the material correspond to aluminum cast, which is characterized by Young's modulus of $75,000\ \mathrm{N/mm^2}$, Poisson's ratio of 0.3, and mass density of $2700\ \mathrm{kg/m^3}$. Note that geometric shape of the design space is rather complex due to the prescribed boundary conditions, like bores interfaces, edges and the like. For the mode-based dynamic response computation, an overall modal

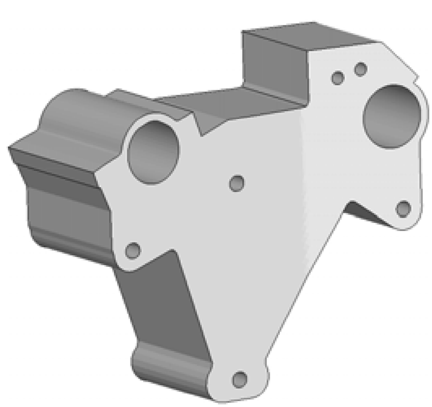

Fig. 8 Full designable domain.

Fig. 9 Layout solution after smoothing.

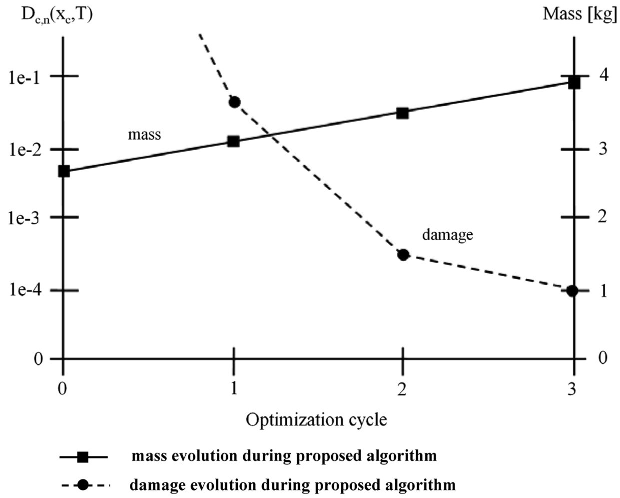

Fig. 10 Damage evolution with respect to additional mass.

damping ration of 5% has been used and the necessary predefined parameters used for the optimization are defined as

$$b_{p=0} = 2700\ \mathrm{kg/m^3}, \quad V_0 = 0.165 \cdot V_\Omega, \quad \beta_1 = \beta_2 = \beta_3 = 0.025$$

$$D_{\mathrm{user}} = 1.0\mathrm{e}-4, \quad T = 18\ \mathrm{s}, \quad q = 7600$$

After three cycles the iterative optimization process is successfully terminated. The final structure occupies 24% of the original design domain. Figure 9 shows the final result after an automatically preformed smoothing of the shape of the obtained design.

Figure 10 contains a diagram that indicates the successive decrease of a meaningful damage. Note that the ordinate for $D_{c,n}$ is logarithmic.

The latter optimization has been performed in order to compare the results with an already existing and implemented bracket, which was designed without topology optimization. The damage of the optimized structure decreases, for the same weight, about a factor of 1000 with respect to the implemented design (from 0.1 to 1.0e − 4).

The entire optimization procedure needed approximately 50 h of CPU time. Each dynamic response computation has been performed on an Intel Pentium 4 processor with 3 GHz. All other computations have been performed on standard UNIX/Linux workstations. However, the conventional design loop needed several weeks.

V. Conclusions

In the proposed algorithm for dynamic topology optimization, damage is used as natural termination criterion of the iterative optimization procedure, as well as for the determination of a single meaningful ESL. This enables the formulation of an efficient algorithm for structural optimization of huge and dynamically loaded FE models. The numerical examples show either a good correlation with previously reported examples or a significant improvement in terms of structural damage. An industrial example (Sec. IV.D) underlines that the proposed algorithm enables the optimization of large and complex structures undergoing transient deformations.

Acknowledgments

Support of this work in the framework of the K2-Austria Center of Competence in Mechatronics (ACCM) and the Engineering Center Steyr of Magna Powertrain is gratefully acknowledged.

References

[1] Bendsøe, M. P., and Kikuchi, N., "Generating Optimal Topologies in Structural Design Using a Homogenization Method," *Computer Methods in Applied Mechanics and Engineering*, Vol. 71, 1988, pp. 197–224.
doi:10.1016/0045-7825(88)90086-2

[2] Bendsøe, M. P., "Optimal Shape Design as a Material Distribution Problem," *Structural and Multidisciplinary Optimization*, Vol. 1, No. 4, 1989, pp. 193–202.
doi:10.1007/BF01650949

[3] Leiva, J. P., Watson, B. C., and Kosaka, I., "Modern Structural Optimization Concepts Applied to Topology Optimization," *40th AIAA/ASME/ASCE/AHS/ASC Structures, Structural Dynamics, and Material Conference*, AIAA, Reston, VA, 1999, pp. 1589–1596.

[4] Bendsøe, M. P., and Sigmund, O., "Material Interpolation Schemes in Topology Optimization," *Archive of Applied Mechanics*, Vol. 69, 1999, pp. 635–654.
doi:10.1007/s004190050248

[5] Bendsøe, M. P., and Kikuchi, N., "Generating Optimal Topologies in Structural Design Using a Homogenization Method," *Computer Methods in Applied Mechanics and Engineering*, Vol. 71, No. 2, 1988, pp. 197–224.
doi:10.1016/0045-7825(88)90086-2

[6] Nishiwaki, S., Frecker, M. I., Min, S., and Kikuchi, N., "Topology Optimization of Compliant Mechanisms Using the Homogenization Method," *International Journal for Numerical Methods in Engineering*, Vol. 42, 1998, pp. 535–559.
doi:10.1002/(SICI)1097-0207(19980615)42:3<535::AID-NME372>3.0.CO;2-J

[7] Rozvany, G. I. N., Zhou, M., and Birker, T., "Generalized Shape Optimization Without Homogenization," *Structural and Multidisciplinary Optimization*, Vol. 4, Nos. 3–4, 1992, pp. 250–252.
doi:10.1007/BF01742754

[8] Zhou, M., and Rozvany, G. I. N., "The COC Algorithm. Part II: Topological, Geometrical, and Generalized Shape Optimization," *Computer Methods in Applied Mechanics and Engineering*, Vol. 89, 1991, pp. 309–336.
doi:10.1016/0045-7825(91)90046-9

[9] Eschenauer, H. A., and Olhoff, N., "Topology Optimization of Continuum Structures: A Review," *Applied Mechanics Reviews*, Vol. 54, No. 4, 2001, pp. 331–389.
doi:10.1115/1.1388075

[10] Fox, R. L., and Kapoor, M. P., "Structural Optimization in the Dynamics Response Regime—A Computational Approach," *AIAA Journal*, Vol. 8, No. 10, 1970, pp. 1798–1804.
doi:10.2514/3.5993

[11] Diaz, A. R., and Kikuchi, N., "Solutions to Shape and Topology Eigenvalue Optimization Problems Using a Homogenization Method," *International Journal for Numerical Methods in Engineering*, Vol. 35, 1992, pp. 1487–1502.
doi:10.1002/nme.1620350707

[12] Kang, B. S., Choi, W. S., and Park, G. J., "Structural Optimization Under Equivalent Static Loads Transformed from Dynamic Loads Based on Displacement," *Computers and Structures*, Vol. 79, No. 2, 2001, pp. 145–154.
doi:10.1016/S0045-7949(00)00127-9

[13] Choi, W. S., and Park, G. J., "Transforming of Dynamic Loads into Equivalent Static Loads Based on Modal Analysis," *International Journal for Numerical Methods in Engineering*, Vol. 46, 1999, pp. 29–43.
doi:10.1002/(SICI)1097-0207(19990910)46:1<29::AID-NME661>3.0.CO;2-D

[14] Choi, W. S., and Park, G. J., "Structural Optimization Using Equivalent Static Loads at All Time Intervals," *Computer Methods in Applied Mechanics and Engineering*, Vol. 191, Nos. 19–20, 2002, pp. 2105–2122.
doi:10.1016/S0045-7825(01)00373-5

[15] Kang, B. S., Park, G. J., and Arora, J. S., "Optimization of Flexible Multibody Dynamic Systems Using the Equivalent Static Load Method," *AIAA Journal*, Vol. 43, No. 4, 2005, pp. 846–852.
doi:10.2514/1.4294

[16] MSC.Adams, Software Package, Ver. 2005.2.0, MSC Software, Santa Ana, CA, 2005.

[17] FEMFAT, Software Package, Ver. 4.7, Engineering Center Steyr, St. Valentin, Austria, 2009.

[18] Rozvany, G. I. N., "Aims, Scope, Methods, History and Unified Terminology of Computer-Aided Topology Optimization in Structural Mechanics," *Structural and Multidisciplinary Optimization*, Vol. 21, No. 2, 2001, pp. 90–108.
doi:10.1007/s001580050174

[19] Choi, W. S., Park, K. B., and Park, G. J., "Calculation of Equivalent Static Loads and Its Application," *Nuclear Engineering and Design*, Vol. 235, No. 22, 2005, pp. 2337–2348.
doi:10.1016/j.nucengdes.2005.05.030

[20] Sigmund, O., "A 99 Line Topology Optimization Code Written in MATLAB," *Structural and Multidisciplinary Optimization*, Vol. 21, No. 2, 2001, pp. 120–127.
doi:10.1007/s001580050176

[21] Pedersen, P., "Influences from Non-Linearities on Optimal Shape Design," *7th AIAA/USAF/NASA/ISSMO Symposium on Multidisciplinary Analysis and Optimization*, AIAA, Reston, VA, 1998, pp. 1123–1130; also AIAA Paper 98-4853.

[22] Pedersen, P., "Some General Optimum Design Results Using Anisotropic, Power Law Nonlinear Elasticity," *Structural and Multidisciplinary Optimization*, Vol. 15, No. 2, 1998, pp. 73–80.
doi:10.1007/BF01278492

[23] Lemaitre, J., *A Course on Damage Mechanics*, 2nd ed., Springer–Verlag, Berlin, 1996.

[24] Lemaitre, J., and Chaboche, J.-L., *Mechanics of solid materials*, Cambridge Univ. Press, Cambridge, England, U.K., 1990, Chap. 7.

[25] Haibach, E., *Betriebsfestigkeit:Verfahren und Daten zur Bauteilberechnung*, VDI–Verlag, Düsseldorf, Germany, 1984, Chap. 3.

[26] Eichelseder, W., "Rechnerische Lebensdaueranalyse von Nutzfahrzeugkomponenten mit der Finiten Elemente Methode," Ph.D. Thesis, Univ. of Technology, Graz, Austria, 1989.

[27] Gaier, C., and Dannbauer, H., "Fatigue Analysis of Multiaxially Loaded Components with the FE-Postprocessor FEMFAT-MAX," *Biaxial/Multiaxial Fatigue and Fracture*, edited by A. Carpinteri, M. De Freitas, and A. Spagnoli, Elsevier Science, Oxford, 2003, pp. 223–240.

[28] Dannbauer, H., Dutzler, E., and Eichelseder, W., "Leichtbau Durch Strukturoptimierung auf Basis von Betriebsfestigkeitskennwerten," *MP Materials Testing*, Nos. 7–8, 2005, pp. 440–445.

[29] Grün, F., "Form- und Topologieoptimierung Unter Berücksichtigung der Betriebsfestigkeit," M.S. Thesis, Montan Univ., Leoben, Austria, 2002.

[30] Sherif, K., "Topologieoptimierung Dynamisch und Komplex Belasteter Bauteile," M.S. Thesis, Johannes Kepler Univ., Linz, Austria, 2008.

[31] Fischer, P., and Witteveen, W., "Integrated MBS-FE-Durability Analysis of Truck Frame Components by Modal Stresses," *15th European Adams Users' Conference*, MSC Software, Santa Ana, CA, 2000, http://www.mscsoftware.com/support/library/conf/adams/euro/2000/Steyr_Durability_Truck_Frame.pdf [retrieved 27 April 2010].

[32] Park, G. J., Kang, B. S., and Choi, W. S., "Validation of a Structural Optimization Algorithm Transforming Dynamic Loads into Equivalent Static Loads," *Journal of Optimization Theory and Applications*, Vol. 118, No. 1, 2003, pp. 191–200.
doi:10.1023/A:1024799727258

[33] TOSCA, Software Package, Ver. 5.0, FE-Design, Karlsruhe, Germany, 2004.

[34] Meske, R., Sauter, J., and Schnack, E., "Nonparametric Gradient-Less Shape Optimization for Real-World Applications," *Structural and Multidisciplinary Optimization*, Vol. 30, No. 3, 2005, pp. 201–218.
doi:10.1007/s00158-005-0518-0

[35] Mlejnek, H. P., and Schirrmacher, R., "An Engineer's Approach to Optimal Material Distribution and Shape Finding," *Computer Methods in Applied Mechanics and Engineering*, Vol. 106, No. 1–2, 1993, pp. 1–26.
doi:10.1016/0045-7825(93)90182-W

[36] Rozvany, G. I. N., Zhou, M., Birker, T., and Sigmund, O., "Topology Optimization Using Interactive Continuum-Type Optimality Criteria (COC) Methods for Discretized Systems," *Topology Design of Structures*, Kluwer Academic, Dordrecht, The Netherlands, 1993, pp. 273–286.

A. Messac
Associate Editor